

We are IntechOpen, the world's leading publisher of Open Access books Built by scientists, for scientists

4,800

Open access books available

122,000

International authors and editors

135M

Downloads

Our authors are among the

154

Countries delivered to

TOP 1%

most cited scientists

12.2%

Contributors from top 500 universities



WEB OF SCIENCE™

Selection of our books indexed in the Book Citation Index
in Web of Science™ Core Collection (BKCI)

Interested in publishing with us?
Contact book.department@intechopen.com

Numbers displayed above are based on latest data collected.

For more information visit www.intechopen.com



Modelling of Long Period Gratings in Photonic Crystal Fibres and Sensors Based on Them

Jovana Petrovic
University of Oxford¹
United Kingdom

1. Introduction

Optical fibres are a true representative of the remarkable advancements and speed of adoption and commercialisation of technology in recent decades. Propelled by the invention of the laser in 1960, these tiny waveguides quickly spread from the scientific laboratories into the everyday life: Internet, medical diagnostics, sensors in food, transport, oil and other industries, decoration. Application of fibres relies on possibility of controlling the propagation of light through them which has initiated invention of a range of accessories and fibre-based devices. This chapter is dedicated to a widely exploited group of fibre devices called long period gratings.

In general, grating is a periodic change in the refractive index profile along the fibre. Depending on their periods gratings are divided into: fibre Bragg gratings (FBGs) with periods comparable to the wavelength of the guided light and long period gratings (LPGs) with periods ranging from several tens to several hundreds of microns. The former reflect narrow bandwidths and are therefore used as band rejection filters in transmission or retro reflectors. LPGs were first designed (Vengsarkar et al., 1996) to mend the problem of back reflection in FBGs that appears to be detrimental in some applications, e.g. gain equalizers, (Vengsarkar et al., 1996). Due to the dependence of their spectral bands on external parameters both types of gratings are now widely used in sensing technology. In addition to inherited advantages of fibre sensors such as simplicity of interrogation schemes, compactness, multiplexing capability and non-obtrusive interaction with living tissues, gratings exhibit very high sensitivity and localisation of the parameter change, which makes them suitable for biomedical diagnostics, remote sensing in oil, food and pharmaceutical industry and radioactive environments, as well as build-in sensors in transportation.

Advanced laser processing techniques along with mechanical and chemical methods allow for fabrication of LPGs in practically any fibre regardless of its index profile and material composition, Fig. 1a)-c). Therefore, it is not surprising that the major novelty in fibre industry – the photonic crystal fibre (PCF) (Knight et al., 1996; Russell, 2003), was quickly embraced as a new medium for grating fabrication. Different guiding principle of PCFs

¹ Results reported in this chapter are part of the author's PhD thesis produced at the Photonics Research Group at Aston University, UK

introduced new features to LPGs, which opened up new possibilities for sensing applications. For example, the LPG reported in (Dobb *et al.*, 2004) can solve the problem of cross-sensitivity to temperature. Namely, in most grating sensors variations in temperature contribute to the signal in the same way as the changes in other parameters, hence various compensation schemes have to be employed which increases the complexity and cost of the sensor. LPGs fabricated by Dobb *et al.* in endlessly single mode (ESM) PCF by an electric arc are not sensitive to temperature, while they are sensitive to strain, bending and refractive index and therefore represent a simple solution to this problem. It should be noted that the more complex sensors have been reported in which the sensitivity of an LPG to a few parameters has been used for their simultaneous sensing. LPGs in PCFs have also found applications in microfluidics devices. For more information on LPG sensors see (James & Tatam, 2003).

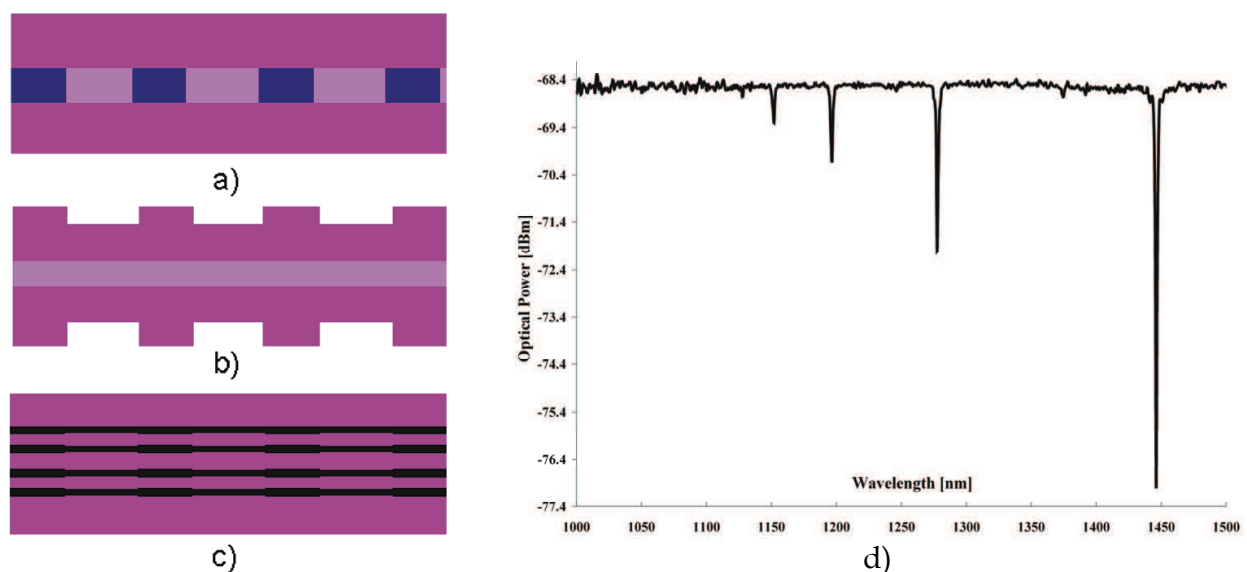


Figure 1. Schematic examples of long period gratings: a) in the core, b) corrugated cladding, c) in PCF. d) Example of grating transmission spectrum (produced by T. Allsop)

In order to fully understand and exploit the potential of LPGs in PCFs the theoretical study and practical models are needed. Naturally, the consideration is based on previous independent extensive studies of LPGs (Erdogan, 1997 a); Kashyap, 1999; Othonos & Kalli, 1999) and PCFs (Birks, 1997; Russel, 2003), to name just a few. The coupled-mode theory (CMT) of fibre gratings (Erdogan, 1997 a) has been the most widely applied model of LPGs, largely due to the relatively simple physical picture based on the phase matching condition. Due to the complex geometry of PCF, accurate simulations of the mode profiles of PCFs require numerical methods, while analytical methods imply calculation of the effective refractive index of the photonic crystal (Park *et al.*, 2006). Various numerical methods have been successfully applied: plain wave expansion method (Ferrando *et al.*, 1999), beam propagation method (Eggleton *et al.*, 2000), full-vectorial finite difference method (Zhu *et al.*, 2002), finite element method (Uranus & Hoekstra, 2004). In this chapter a method based on conjuncture of CMT and finite elements that allows for analysis of spectra and sensitivity of LPGs in PCFs of various geometries is presented.

Section 2 introduces the physical model of LPG and its numerical implementation, and is followed by a detailed example of the application of the model to the temperature

insensitive LPG in Section 3. The analysis of the grating spectrum and resonant modes is further used to calculate grating sensitivity to temperature and strain. The final subsection is dedicated to the application of the model to reverse engineering of the grating index profile. Applications and practical limitations of the model are discussed in Section 4. Finally, Section 5 summarises results and suggests directions for future work.

2. Numerical Model

2.1 The Physics of Long Period Gratings

Periodic perturbation of the index profile of the fibre that defines fibre grating acts as a resonant scatterer on the incoming core mode. In consequence, the core mode periodically couples to other co- and counter-propagating fibre modes. The former is characteristic of the long period grating and the latter of the fibre Bragg grating, the difference stemming from a large difference in periods of these gratings. The vector sum of the propagation vector of the core mode and the reciprocal grating vector defines the propagation vector of the resonant mode. If the grating period is long enough its vector is shorter than the propagation vector of the core mode, and the coupled modes are copropagating. The opposite is the case for the short period grating (FBG). Both cases are shown in Fig. 2. These are the most commonly used scenarios; for the full description see (Erdogan, 1997 a).

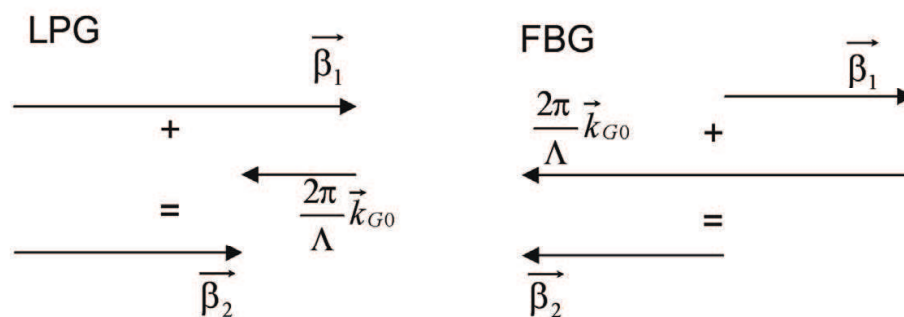


Figure 2. Phase matching in long period grating (left) and fibre Bragg grating (right)

Cladding modes excited by an LPG are irradiated at the interface between cladding and surrounding medium, which causes the losses observed as attenuation bands in the spectrum, Fig. 1d). Resonant wavelengths are determined by the grating period and the order of the cladding mode. Coupling strength of the grating depends on overlap of the electric fields of the core and resonant cladding modes across the grating and the grating refractive index. It determines the magnitude of attenuation bands, the so called 'grating strength'.

2.2 Mathematical Model of the Long Period Grating

Given that it consists of a small change in the index profile of the fibre, an LPGs can be successfully treated by the perturbation theory, the adaptation of which to resonant systems is known as the coupled mode theory (CMT). It assumes that each mode excited by the grating can be represented as a linear combination of the eigenmodes of the unperturbed

fibre. The wavelength at which the coupling to a specific cladding mode occurs is given by the phase matching condition

$$\lambda = (n_{co}^{eff} - n_{cl}^{eff})\Lambda_B = \delta n^{eff} \Lambda \quad (1)$$

where n_{co}^{eff} and n_{cl}^{eff} are the effective mode indices of the core and cladding modes respectively, Λ is the beat length and λ is the resonant wavelength. This condition allows for the representation of the excited mode by one eigenmode of the fibre, thereby reducing the problem to the system of two coupled mode equations

$$\frac{dA_{co}(z)}{dz} = i\kappa_{co-co}A_{co}(z) + i\frac{s}{2}\kappa_{co-cl}A_{cl}(z)e^{-i2\delta z} \quad (2)$$

$$\frac{dA_{cl}(z)}{dz} = i\kappa_{cl-co}A_{co}(z)e^{i2\delta z} + i\frac{s}{2}\kappa_{cl-cl}A_{cl}(z) \quad (3)$$

where A_{co} and A_{cl} are the slowly varying amplitudes of the core and cladding modes, κ_{co-co} , κ_{cl-cl} and $\kappa_{co-cl} = \kappa_{cl-co}^*$ are the coupling coefficients, s is the grating modulation depth and $\delta = \pi\left(\frac{n_{co}^{eff} - n_{cl}^{eff}}{\lambda} - \frac{1}{\Lambda}\right)$ is the detuning from the resonant wavelength. The coupling is determined by the transverse fields of the resonant modes $\mathbf{E}(\mathbf{r})$ and the average index of the grating $\Delta n(\mathbf{r})$

$$\kappa_{ij} = \frac{\omega\epsilon_0 n}{4} \int \Delta n(\mathbf{r})\mathbf{E}_i(\mathbf{r})\mathbf{E}_j^*(\mathbf{r})d\mathbf{r} \quad (4)$$

Here, the electric fields of the modes are normalised so that each mode carries 1W of power. Whereas the mode field profiles of the circularly symmetric fibres are well known, the modal analysis of PCFs is more demanding and requires numerical methods. System (2-3) is then readily solved to obtain the field amplitudes of the coupled modes along the fibre for a given wavelength (Snyder & Love, 2000; Erdogan, 1997 a).

Grating resonances are best visualised by constructing the grating characteristics -- a family of curves $\Lambda(\lambda)$ for different cladding modes over a range of wavelengths. Resonant wavelengths are then found in intersections of these curves and the line $\Lambda=L$ representing the beat length equal to the grating period L . In general case, the grating is not perfectly sinusoidal, and the higher order terms in the Fourier transform of its refractive index must be taken into account. This results in the resonant condition $\Lambda=L/N$ for the N th order grating (Kashyap, 1999).

For the gratings with weak index modulation and narrow attenuation bands two-mode description is usually sufficient. These conditions are fulfilled in the majority of practical applications.

2.3 Numerical Model of the Photonic Crystal Fibre

The starting point in the fibre grating analysis is the characterisation of the modes supported by the fibre. PCFs studied here have a hexagonal 'holy' photonic crystal as the inner cladding and a solid core produced by omitting the central hole. These fibres have been represented by the model based on the effective refractive indices of the core and the photonic crystal cladding (Russell, 2003). Due to the presence of air holes effective index of the cladding is lower than the index of the core, which keeps the light confined to the core. However, the analogy with the step-index fibres is not complete as there is no clear boundary between the core and the cladding. Due to the complex geometry of PCFs and the high refractive index contrast between the pure silica and air holes, modes of these fibres are most accurately calculated by solving Maxwell's equations by a full-vectorial numerical solver. A comparison of the different numerical methods used to study PCFs can be found in (Uranus & Hoekstra, 2004). A problem in hand imposes additional constraints on the choice of the method. In our case, the analysis of LPG in air and its sensitivity to the refractive index of the surrounding medium, precludes the use of methods that assume infinite photonic crystal, e.g. the super-lattice method. As opposed to the typical problems of nonlinear optics and transmission, which are mainly concerned with the propagation of the core mode, the intrinsic property of LPG to couple the core to the cladding modes requires accurate calculation of the propagation constants and field profiles of many modes in the whole fibre cross section. Here we choose the finite element method which meets both requirements and offers additional benefits of simulating fibres of different geometries and fibres with random variations in hole diameters. The calculations were performed by the commercial software Comsol 3.1 (COMSOL AB).

Eigenmodes and their effective indices were found by simulating the cross section of the fibre with the jacket removed and surrounded by air. The necessary resolution of the mesh in the photonic crystal was achieved by exploiting the fibre symmetry. Criteria for the choice of mesh parameters were convergence and accuracy of the effective refractive index.

2.4 Models of Grating Sensitivity

Long period grating response to the change in external parameter is observed as a shift in the resonant wavelength or/and as a change in magnitude or shape of the attenuation bands. In most cases, changes in temperature, strain and the refractive index lower than the index of fibre cladding cause wavelength shift, while bending and changes in refractive index to the values higher than the index of the fibre cladding cause changes in shape and magnitude of attenuation bands. In the former case, the grating sensitivity to parameter X can be calculated by linearisation of the grating characteristic of the resonant mode around the resonant wavelength and is given by expression

$$\frac{\partial \lambda}{\partial X} = \gamma \left(\frac{\partial \Lambda}{\partial X} \delta n^{eff} + \frac{\partial \delta n^{eff}}{\partial n} \frac{\partial n}{\partial X} \Lambda \right). \quad (5)$$

$$\gamma = \frac{1}{1 - \frac{d \delta n^{eff}}{d \lambda} \Lambda} = \frac{1}{\delta n^{eff}} \frac{d \lambda}{d \Lambda} \quad (6)$$

The generalised sensing parameter γ is defined in (MacDougall et al., 1998; Shu et al., 2002) and accounts for the effects of the material and waveguide dispersion of the fibre, $\delta n^{eff} = \delta n^{eff}(\lambda(X), n(\lambda(X), X))$. The rightmost term in (6) shows a direct relation between γ and the slope of the grating characteristic. As the derivatives in the above equations are obtained numerically, this method will be referred to as semi-analytical.

Change in an external parameter can have two major effects on an LPG: change in the grating period and in the refractive index of the fibre. If the index change is incorporated in the model of the PCF and the resonant wavelength found using the new grating period, the approximation made in the linear model is eliminated. Graphic representation of this solution distinguishes contributions of each effect as will be shown in the next Section. This method will be referred to as numerical.

The most important assumptions made in the model are that the index change in the grating is small and that the symmetry of the fibre is preserved. The profile of the grating and the fibre itself are not restricted in any other way. Moreover, constraints imposed by symmetry can be dropped at the expense of the mesh quality and the calculation time. Nonuniform grating can be treated by transfer matrix method that uses CMT to evaluate transmission matrix of each uniform part. Therefore, the suggested numerical model of the wavelength shift based sensitivity applies to a vast majority of LPGs in practical use today.

2.5 Reverse Engineering of the LPG from its Spectrum

In this section we consider an actual index profile of the grating in more detail. The general types of perturbation are: (i) change in the refractive index of the waveguide and (ii) changes in the geometry of the fibre such as the change in hole radii, tapering, corrugation, Fig. 1a)-c). Whereas gratings written in step-index fibres usually consist of the change in the refractive index of the photosensitive core, gratings written in PCFs are slightly more complicated. They comprise change in the refractive index across the fibre cross-section and the change in the geometry of the PCF, for example squeezing of holes induced by the strong electric-arc (Morishita & Miyake, 2004). As the waveguiding principle of PCF lifts the requirement for the photosensitive core, all parts of the fibre can be made of the same material (usually silica) which makes them equally sensitive to the writing technique. Moreover, light scattering on the holes impairs precise focusing into the core of the PCF. Structure of the gratings in PCFs has been a subject of several studies, e.g. (Humbert & Malki, 2002; Fotiadi et al., 2007). Here we describe method for nondestructive analysis of the grating profile based on spectral data taken during the grating fabrication. The idea behind the analysis is to establish a connection between the parameters of the induced index profile and the grating property which can be measured in a way that generates enough data to extract these parameters but that does not affect grating performance. The measurement of the dynamics of grating transmission spectrum during the fabrication is recognised as suitable since it is easily recorded and contains signatures of the values of coupling coefficients and detuning for a range of grating lengths.

According to the CMT, grating transmission is a function of the coupling coefficients defined by (4). In its simplest form, which assumes that the detuning from the resonant wavelength is balanced by the dc coupling, the expression for the grating transmission is given by

$$T(z) = \cos^2(\kappa z) \quad (7)$$

Cross coupling coefficient κ depends on the grating index profile and field profiles of the resonant modes. By averaging the index change in the photonic crystal, integral in (4) can be replaced by the sum of contributions of the core (co), photonic crystal (pc) and the outer cladding (cl) of the fibre

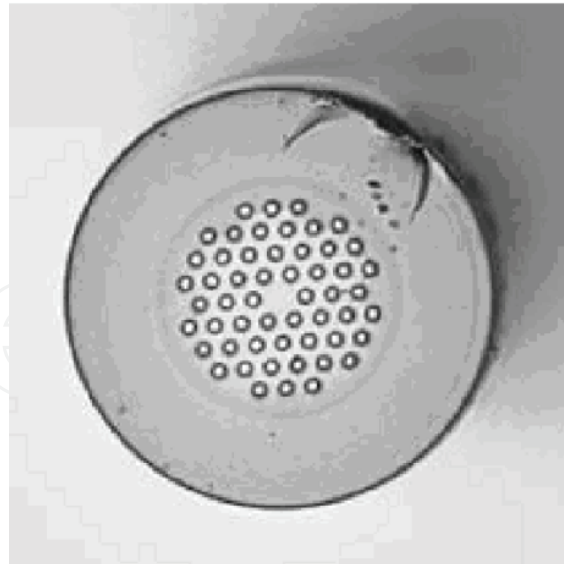
$$\kappa = \frac{\omega \epsilon_0 n}{4} \sum_{j=co,pc,cl} I_j^{co-cl} \Delta n_j \quad (8)$$

where I_j^{co-cl} is the overlap integral of the normalised core and cladding modes and Δn_j is the overall refractive index change in the j part of the fibre. The domains of the fibre cross section are defined purely geometrically and not in the relation to the spatial extent of fibre modes. It is assumed that the grating profile consists of the change in hole radius ΔR_h and the refractive index of silica Δn . As the change in the size of holes does not significantly affect core nor cladding, $\Delta n_{co} = \Delta n_{cl} = \Delta n$. On the other hand, Δn_{pc} is calculated by averaging the contributions of the air and silica to the dielectric constant of the photonic crystal. The best fit of the calculated minimal transmission to the maximum of the attenuation band for different grating lengths gives the parameters ΔR_h and Δn . This model reflects the guiding principle of the studied PCF. Nevertheless, it should be noted that the average index of the photonic crystal that features in our model is not equivalent to the effective index of the crystal used in the model of ESM PCF in (Birks et al., 1997), as the latter is based on the propagation constant of the fundamental space-filling mode of the photonic crystal.

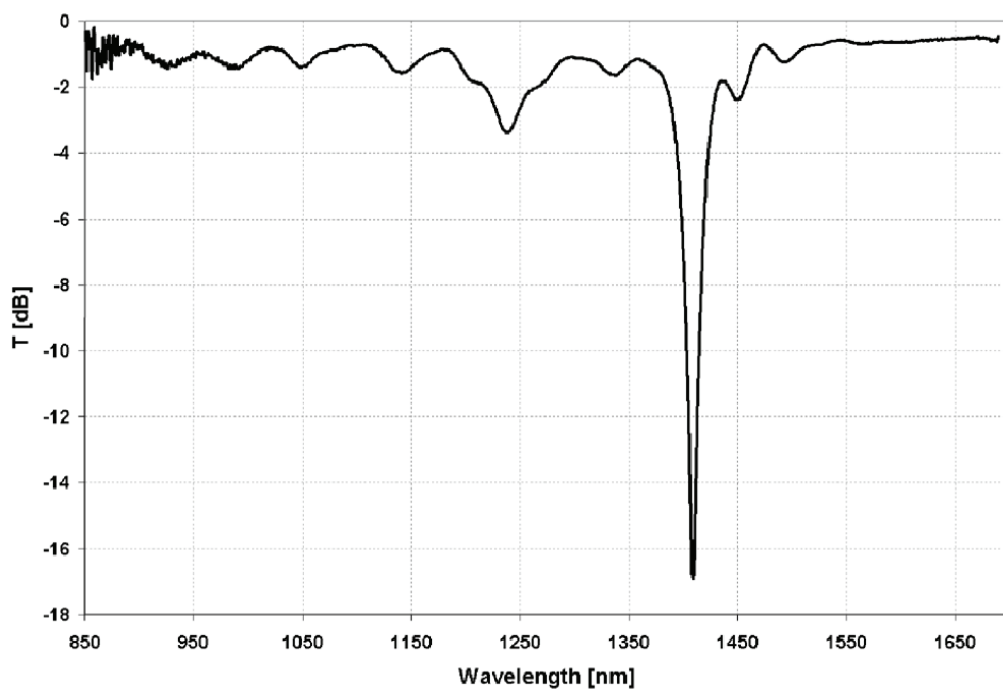
3. Example: LPG in PCF fabricated by Electric Arc

3.1 Description of the device

Long period grating in endlessly single mode ESM 1550-01 PCF reported in (Dobb et al., 2004) is studied as an original example of the grating insensitive to temperature and simultaneously sensitive to other external parameters. The fibre was made from pure silica with four rings of hexagonally arranged air holes with the space between adjacent holes being $8\mu\text{m}$. The central hole was omitted to form the core, Fig. 3a). The filling factor was 0.46. A series of LPGs with different periods were inscribed by exposing the PCF to the electrical discharge provided by a commercial splicer (Fitel S175 v2000) (Dobb et al., 2006). A detailed inspection of the grating by the phase microscope did not reveal any change in the hole size. The LPG with period $500\mu\text{m}$ and length 25.5mm is studied in detail. Its transmission spectrum, shown in Fig. 3b), features two pronounced attenuation bands at 1402nm and 1239nm . Increase in the grating period causes a blue shift in the wavelength spectrum, in contrast to LPG behaviour in conventional single mode fibre, but similar to other LPGs in PCFs (Morishita & Miyake, 2004). Since neither the grating spectrum nor the bending sensitivity indicated any birefringence, the original hexagonal symmetry of the fibre was considered unaffected by the electric arc.



a)



b)

Figure 3. a) Cross section of ESM 1550-01 PCF. b) Transmission spectrum of an LPG fabricated in this fibre by electric arc (Dobb et al., 2004)

3.2 Grating Spectrum and Resonant Modes

Calculation of the modes of ESM-1550 PCF is facilitated by its hexagonal symmetry. It belongs to the so called C_{6v} symmetry group, which means that its modes can be divided into eight symmetry classes: non-degenerate classes 1, 2, 7, 8 with the irreducible zone angle of $\pi/6$ and degenerate classes 3, 4, 5, 6 with the irreducible zone angle of $\pi/2$. Four classes in each group are the result of permutations of the two boundary conditions: perfect magnetic

conductor - $\vec{n} \times \vec{H} = 0$ and perfect electric conductor - $\vec{n} \times \vec{E} = 0$, (McIsaac, 1975). The effective index of the core mode was calculated with the accuracy better than $2 \cdot 10^{-7}$ and the effective indices of cladding modes with the accuracy better than 10^{-6} . Examples of fibre modes and irreducible zones are shown in Fig. 4.

Modal map of the fibre is used to construct the grating characteristic shown in Fig. 5. It confirms the experimental observation that an increase in the grating period causes blue shift in the resonant wavelength. In the given wavelength range such behaviour is characteristic of PCFs and has been explained in (Morishita & Miyake, 2004). Resonant wavelengths of the first order grating are found at intersections of these curves with the line $\Lambda=L$, where L is the grating period. Fig. 4b) shows the intensity profile of the quasi LP mode that has been identified as resonant at 1402nm.

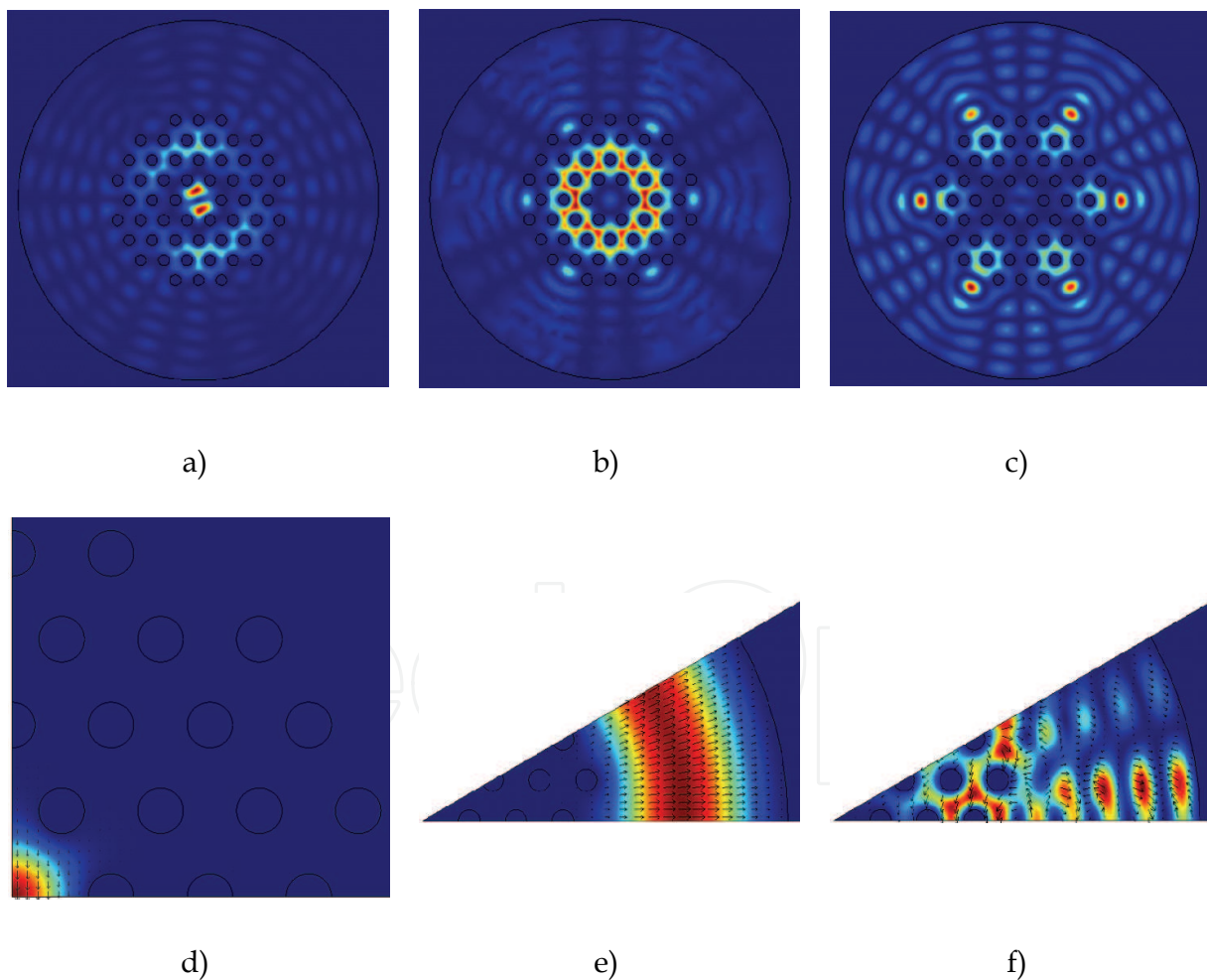


Figure 4. Modes of ESM PCF. a), b), c) - examples of modes guided by different parts of the fibre. d), e), f) illustrate irreducible zones of the fibre. Core mode in d) belongs to a degenerate class while modes in e) and f) belong to non-degenerate classes

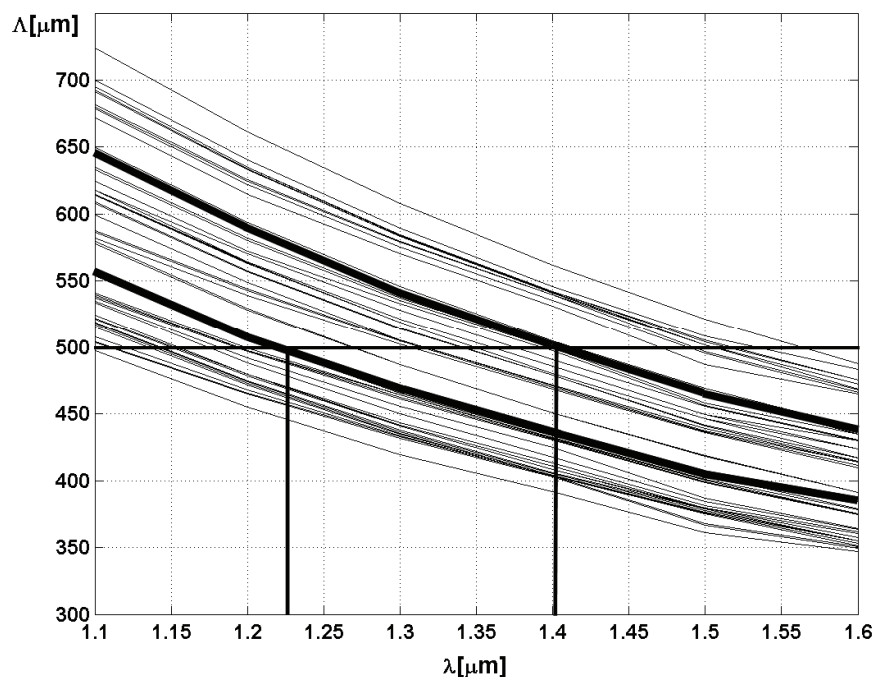


Figure 5. Characteristic of the LPG in ESM 1550-01 PCF. The resonances marked by the vertical lines correspond to the attenuation bands at 1239nm and 1402nm shown in Fig. 3b). Characteristic curves of the resonant modes are emphasized by thick lines

3.3 Grating Sensitivity

3.3.1 Sensitivity to Strain

Expression for the sensitivity to strain was derived from (5) by substitution of X by the linear strain $\varepsilon \equiv \delta\varepsilon = \Delta\Lambda/\Lambda = \Delta L/L$ and is given by

$$\frac{\partial\lambda}{\partial\varepsilon} = \gamma\lambda\left(1 + \frac{\partial\delta n^{eff}}{\partial n} \frac{\eta_\varepsilon}{\delta n^{eff}}\right) \quad (9)$$

The strain-optic coefficient η_ε accounts for the change in the refractive index of the fibre due to the applied strain. It was derived from the change in the optical indicatrix for the field polarized perpendicularly to the direction of the applied strain (Hocker, 1979), $\eta_\varepsilon = -0.5n^3(p_{12} - \mu(p_{12} + p_{11}))$ where $p_{11} = 0.121$ and $p_{12} = 0.27$ are elements of the strain-optic tensor (Guenther, 1990) and $\mu = 0.17$ is the Poisson's coefficient for pure fused silica. The calculated sensitivity to strain was $-1.57\text{nm}/\text{m}\varepsilon$.

The numerical solution was based on the change in the refractive index of silica caused by the maximal strain applied in the experiment $\varepsilon_{\text{max}} = 2\text{m}\varepsilon$. The beat length of the strained fibre was calculated in the range of 8nm around the resonant wavelength. The new resonant wavelength was found by interpolation of the Λ curves at the points determined by the new grating period $\Lambda = L(1 + \varepsilon)$. From Fig. 6 it can be seen that both the contribution from the elongation of the grating and from the strain-optic effect lead to a blue wavelength shift, the former having the major effect.

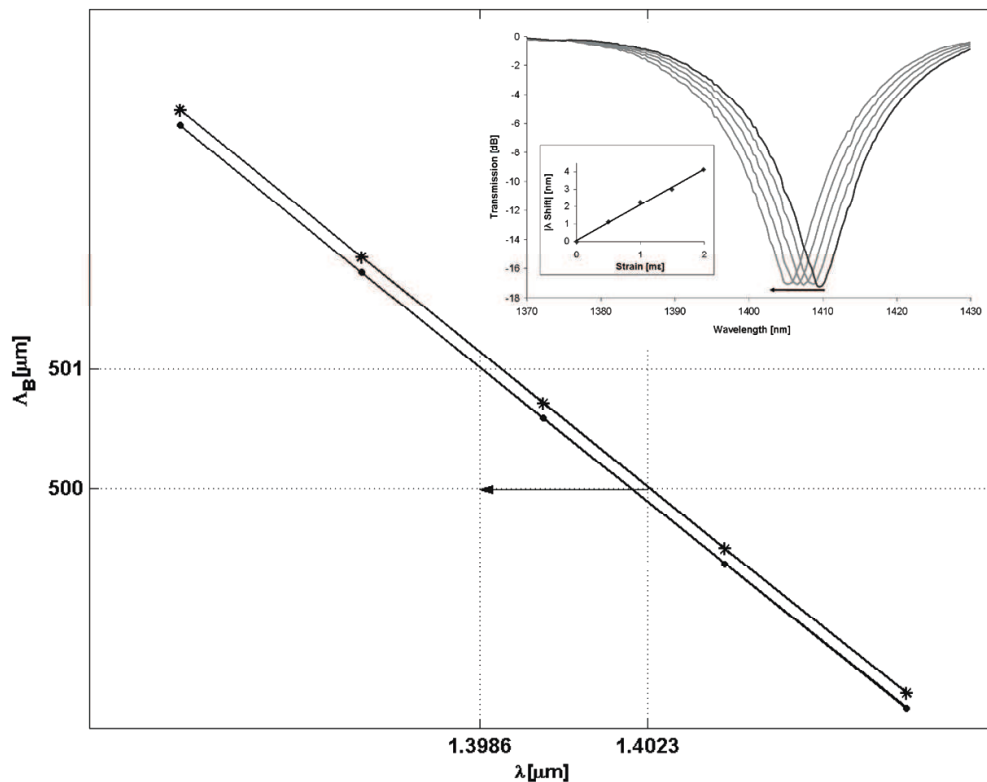


Figure 6. Numerical solution for the shift in the resonant wavelength of the LPG in ESM PCF due to the applied strain. * - unstrained fibre, • - fibre under strain of 2 mε. Arrow - overall wavelength shift. Inset: Measured sensitivity to strain (Dobb et al., 2004)

The model was validated by comparison to the experimental results. The strain response of the LPG in ESM 1550-01 was linear with the sensitivity of -2.08 ± 0.05 nm/mε, as shown in Fig. 6. The numerical result for the sensitivity of -1.85 nm/mε differs from the measured value by 11%, which is better than the error of the semi-analytical result of nearly 25%. Along with the experimental error of 2.4%, the discrepancy between the theoretical and experimental results can be attributed to several neglected effects: inhomogeneous distribution of strain in the PCF caused by the presence of air holes, change in the geometry of the fibre profile due to strain, dispersion of the strain-optic coefficients and the neglected average change in the refractive index of the grating, (Petrovic et al, 2007 a).

3.3.2 Sensitivity to Temperature

Similarly to strain, the expression for the LPG's sensitivity to temperature is a specific case of the generic expression given by (5)

$$\frac{\partial \lambda}{\partial T} = \gamma \lambda \left(\alpha + \frac{\partial \delta n^{eff}}{\partial n} \frac{\eta_T}{\delta n^{eff}} \right) \quad (10)$$

in which $\alpha = \partial \Lambda / \Lambda \partial T = 5 \cdot 10^{-7} \text{ } ^\circ\text{C}^{-1}$ is the thermal expansion coefficient of silica and $\eta_T = \partial n / \partial T = 7.8 \cdot 10^{-6} \text{ } ^\circ\text{C}^{-1}$ is the thermo-optic coefficient of silica (Hocker, 1979). For the

range of temperatures applied in the experiment (20°C-90°C) the maximal change in the refractive index is $5 \cdot 10^{-4}$, hence under the assumption of linear grating response the derivatives already calculated in the previous section could be used. The semi-analytical model gave sensitivity to temperature of 3.8pm/°C.

The numerical solution was obtained reusing the curves from Fig. 6 and following the steps outlined in the previous section. The calculated change in the grating period of -19.23nm, Fig. 7, corresponds to the sensitivity of 4.0pm/°C.

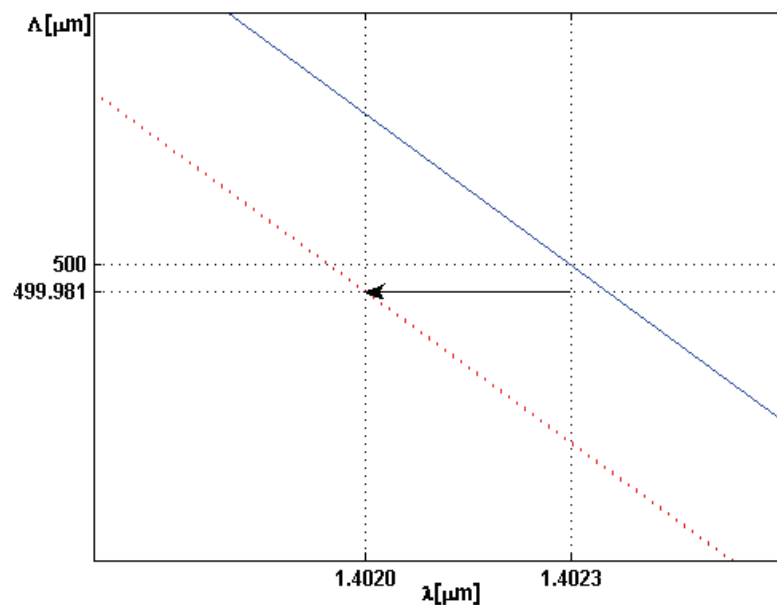


Figure 7. Numerical solution for the sensitivity of the LPG in ESM PCF to temperature. Solid line – grating at the room temperature, dotted line - grating temperature decreased by 77°C. Note the difference in the wavelength shift here and that in Fig. 6

Waveguide dispersion of the resonant mode is such that the thermo-optic effect and the thermal expansion of the fibre cause wavelength shifts of the opposite signs. Although the thermo-optic effect dominates the effect of linear expansion of the fibre, it is itself small because both core and cladding modes are guided mostly through the silica so that their effective indices undergo almost the same change and lead to the small value of the derivative $\partial \delta n^{\text{eff}} / \partial n$. This explains the very low sensitivity of the LPG to temperature reported in (Dobb et al., 2004).

The sign and the order of magnitude of the calculated wavelength shift agree with the experimental result, but the calculated sensitivity overestimates the experimental value $2 \pm 1 \text{ pm}/^\circ\text{C}$. This disagreement is partly due to the large error in the linear regression caused by scattering of the experimental data and partly due to the neglect of the average index change in the model of LPG and linearisation over the large temperature span.

3.4 Reverse Engineering of the Grating Index Profile

The model explained in Section 2.4 was used to find the impact of the electric arc on the ESM PCF. Experimental result of H. Dobb (inset in Fig. 8) shows no wavelength shift during the grating growth. According to the theory in (Erdogan, 1997 b) this justifies application of Eq. (7) to the grating used in this example. Fit of the numerical results to these

measurements gave an estimate of relative decrease in the hole radius of 0.07% and of change in the refractive index of silica of $-3 \cdot 10^{-4}$. The former was confirmed by observation by the phase microscope. The latter can be explained as follows. Decrease in the index of core equals decrease in the index of silica, while the index of cladding decreases less due to the contribution of the air holes to it. Consequently, index difference between the core and the photonic crystal decreases and the confinement of modes weakens causing the increase in overlap of the core and inner cladding modes. This enables coupling between the core and cladding modes necessary for the operation of LPG.

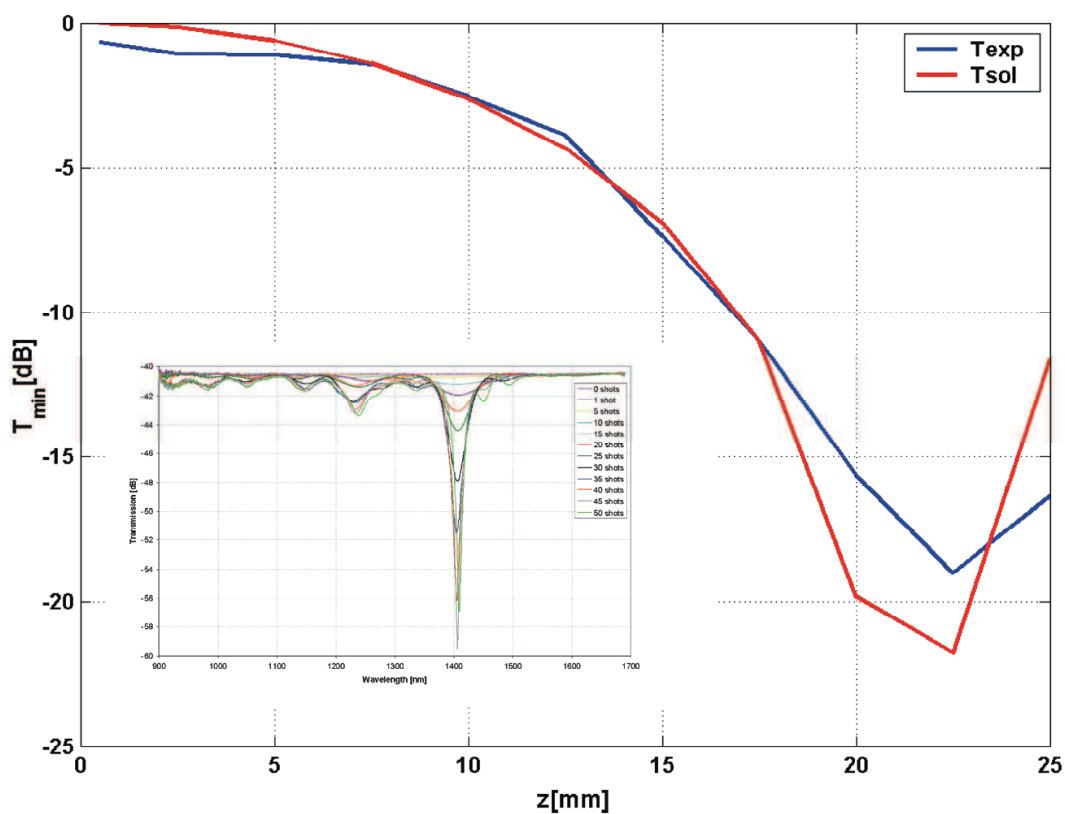


Figure 8. The best fit of the calculated minimal grating transmission (red line) to the experimental result (blue line) vs. grating length. Inset: growth of the LPG spectrum recorded during the grating fabrication by the electric arc

4. Discussion

Without or with minor modifications the described model can be applied to practically any LPG in ESM PCF. Here we assess the generality of the basic model of the grating as well as its further applications in sensing and index profiling.

The calculation of fibre modes and their propagation constants represents the main challenge. Finite element method enables calculation of eigenmodes of fibres with different photonic crystals, fibres with random fluctuations in the hole size that may be introduced during the fabrication process and of asymmetric fibres. Furthermore, the grating characteristic, resonant wavelengths and sensitivity can be reasonably well estimated without knowing the exact grating index profile. The knowledge of the exact grating profile

could be inserted to the model to improve accuracy of these calculations. On the other hand, for the inverse engineering of the grating correct assumption on the induced index change is crucial. If the information on the grating profile is not available, estimate of the index change obtained by averaging explained in Sec. 2.5 can be used in the model of the PCF as a new input condition. As stated above, the geometry of the simulated fibre can be altered easily, hence calculation can be reiterated and the model of grating refined until the match with experiment becomes satisfactory. Incorporation of the problem related physical effects, which are usually neglected at the first instance, can also improve the accuracy of the model. A good example is the sensitivity to strain, the results for which can be refined by taking into consideration the inhomogeneous distribution of strain in the cross section of PCF caused by the presence of the air holes and the dispersion of the strain-optic coefficients.

Implementation of the proposed model is application driven, e.g. for the calculation of the sensitivity based on the wavelength shift the knowledge of the real part of the mode propagation constant is sufficient whereas the calculation of the light power irradiated from the fibre due to the LPG requires knowledge of the complex propagation constant.

Generality of the model is not always desirable as it can lead to ambiguity. Without experimental input, it can be wrongly concluded that all the gratings inscribed in the same fibre with the same period have the same resonant wavelengths. LPGs in PCFs are particularly sensitive to such claims, mainly due to the possible change in the fibre geometry as well as the refractive index which both shift the propagation constants of the fibre. Direct writing, e.g. by femtosecond laser, can easily induce asymmetry in the fibre. If this is ignored, the results will fail to give any information on grating birefringence. Therefore, results obtained from the model should be considered only in conjunction with the information on grating fabrication, measured spectrum and index profile.

5. Conclusion

A general numerical model of long period gratings fabricated in photonic crystal fibres has been presented. It has been illustrated by the example of the grating fabricated by an electric arc in ESM PCF. The generality of the model stems from its capability to simulate LPGs in PCFs of different geometries and composition. Model has been applied to calculate sensitivity of the grating to an external parameter and the examples of temperature and strain sensitivity have been given. To facilitate studies of the structure of these LPGs, the tool has been added to the model, which enables reverse calculation of the parameters of an assumed grating index profile from the recorded growth of grating transmission spectrum during the fabrication. Due to the flexibility of the finite element method the actual index profile of the grating can be easily incorporated into the model. This is particularly important in the calculations of grating strength which requires the calculation of the coupling coefficients, hence the resonant mode profiles.

While the model enables straightforward analysis of a variety of gratings and their sensitivity, its implementation depends on the index profiles of the grating and fibre in hand and its refinement depends on the goal of the study. A general refinement strategy would be to replace the model of unperturbed fibre by the average of perturbed and unperturbed index profiles of the fibre along the grating. However, in practice, measuring the index profile usually implies destroying the device. The procedure for nondestructive index profiling suggested here can be used instead. As its accuracy depends on the model of the index change induced during the grating fabrication, which is based on experimental

observation and measurement, the optimal method should close the loop between the experiment and theory, the loop within which they help and benefit most from each other.

6. Acknowledgement

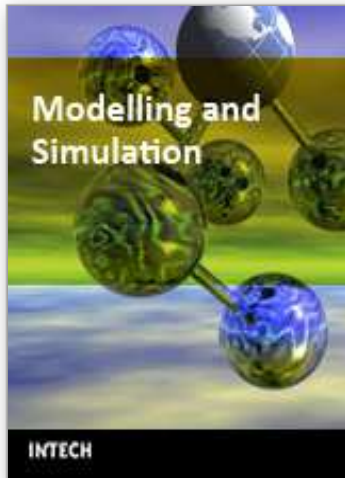
Author would like to thank Vladimir Mezentsev for advice on numerical modelling, Helen Dobb, David Webb and Kyriacos Kalli for discussions and sharing their experimental data, and Thomas Allsop for useful comments and the grating spectrum in Fig. 1d).

7. References

- Birks, T.A.; Knight, J.C. & St. J. Russell, P. (1997) Endlessly single-mode photonic crystal fiber, *Optics Letters*, Vol. , No 13. 961-963
- Dobb, H.; Kalli, K. & Webb, D. J. (2004). Temperature-insensitive long period grating sensors in photonic crystal fibre. *Electronic Letters*, Vol. 40, 657-658
- Dobb, H.; Kalli, K. & Webb, D. J. (2006). Measured sensitivity of arc-induced long-period grating sensors in photonic crystal fibre, *Optics Communications*, Vol. 260, No. 1, 184-191
- Eggleton, B. J.; Westbrook, P. S.; White, C. A.; Kerbage, C.; Windeler, R. S. & Burdge, G. L. (2000). Cladding-Mode-Resonances in Air-Silica Microstructure Optical Fibres. *Journal of Lightwave Technology*, Vol. 18, No. 8, 1084 -1099
- Erdogan, T. (1997). Cladding-mode resonance in short- and long-period fiber grating filters. *Journal of Optical Society of America A*. Vol. 14, No. 8, 1760-1773 a)
- Erdogan, T. (1997). Fiber grating spectra. *Journal of Lightwave Technology*, Vol. 15, No. 8, 1277 - 1294 b)
- Ferrando, A.; Silvestre, E.; Miret, J. J.; Andres, P. & Andres, M. V. (1999) Full-vector analysis of a realistic photonic crystal fiber, *Optics Letters*, Vol. 24, No. 5 , 276-278
- Fotiadi, A. A.; Brambilla; G., Ernst; T., Slattery S. A. & Nikogosyan, D. (2007) TPA-induced long-period gratings in a photonic crystal fibre: inscription and temperature sensing properties, *Journal of Optical Society of America B*, Vol. 24, No. 7, 1475-1480
- Guenther, R. (1990). *Modern Optics*, John Wiley and Sons, Inc.
- Hocker, G. B. (1979). Fiber-optic sensing of pressure and temperature. *Applied Optics*, Vol. 18, No. 9, 1445-1448
- Humbert, G. & Malki, A. (2002) Characterizations at very high temperature of electric arc-induced long-period fiber gratings, *Optics Communications*, Vol. 208, No. 4-6, 329 - 335
- James, S. W. & Tatam, R. P. (2003) Optical fibre long-period grating sensors: characteristics and application. *Measurement Science and Technology*, Vol. 14, No. 5, 49-61
- Kashyap, R. (1999). *Fiber Bragg Gratings*, Academic Press
- Knight, J.C.; Birks, T.A; Russell, P.St.J; & Atkin, D.M. (1996) All-silica single-mode optical fiber with photonic crystal cladding, *Optics Letters*, Vol. 21, No. 19, 1547-1549
- MacDougall, T. W.; Pilevar, S.; Haggans, C. W. & Jackson, M. A. (1998). Generalized expression for the growth of long period gratings. *IEEE Photonics Technology Letters*, Vol. 10, No. 10, 1449-1451
- McIsaac, P. R. (1975). Symmetry-induced modal characteristics of uniform waveguides. I Summary of results. *IEEE Transactions on Microwave Theory Technology*, MTT-23, 421-429

- Morishita, K. & Miyake, Y. (2004) Fabrication and resonance wavelengths of long-period gratings written in a pure-silica photonic crystal fiber by the glass structure change, *Journal of Lightwave Technology*, Vol. 22, No. 1, 625-630
- Vengsarkar, A. M.; Pedrazzani, J. R.; Judkins, J. B.; Lemaire, P. J.; Bergano, N. S. & Davidson, C.R. (1996) Long-period fibre-grating-based gain equalizers. *Optics Letters*, Vol. 21, No. 5, 336-338
- Othonos, A. & Kalli, K. (1999). *Fiber Bragg Gratings*, Artech House Inc.
- Park, K. N.; Erdogan T. & Lee, K. S. (2006) Cladding mode coupling in long-period gratings formed in photonic crystal fibres. *Optics Communications*, Vol 256, No. 2, 541-545
- Petrovic, J. S.; Mezentsev, V.; Dobb, H.; Kalli, K.; Webb, D. J. & Bennion, I. (2007) Sensitivity of LPGs in PCFs Fabricated by an Electric Arc to Temperature, Strain, and External Refractive Index. *Journal of Lightwave Technology*, Vol. 25, No. 5, 1306-1312 a)
- Petrovic, J. S.; Webb, D. J.; Dobb, H.; Mezentsev, V.; Kalli, K. & Bennion, I. (2006). Nondestructive Index Profiling of Long Period Gratings in Photonic Crystal Fibres. *Optical and Quantum Electronics*, Vol. 38, No. 9-11, 913-920 b)
- Russell, P. (2003). Photonic Crystal Fibres. *Science*, Vol. 299, 358-362
- Shu, X.; Zhang, L. & Bennion, I. (2002). Sensitivity characteristics of long-period fiber gratings. *Journal of Lightwave Technology* Vol. 20, No. 2, 255-266
- Snyder, A.W. & Love, J.D. (2000). *Optical Waveguide Theory*, Kluwer Academic Publishers
- Uranus, H. P. & Hoekstra, H. J. W. M. (2004). Modelling of microstructured waveguides using a finite-element-based vectorial mode solver with transparent boundary conditions, *Optics Express*, Vol. 12, No. 12, 2795-2809
- Vengsarkar, A. M.; Lemaire, P. J.; Judkins, J. B.; Bhatia, V.; Erdogan T. & Sipe, J. E. (1996). Long-period gratings as band-rejection filters. *Journal of Lightwave Technoogy*, Vol. 14, No. 1, 58-65
- Zhu Z. & Brown, T. G. (2002). Full-vectorial finite-difference analysis of microstructured optical fibres. *Optics Express*, Vol. 10, No. 17, 853-864

IntechOpen



Modelling and Simulation

Edited by Giuseppe Petrone and Giuliano Cammarata

ISBN 978-3-902613-25-7

Hard cover, 688 pages

Publisher I-Tech Education and Publishing

Published online 01, June, 2008

Published in print edition June, 2008

This book collects original and innovative research studies concerning modeling and simulation of physical systems in a very wide range of applications, encompassing micro-electro-mechanical systems, measurement instrumentations, catalytic reactors, biomechanical applications, biological and chemical sensors, magnetosensitive materials, silicon photonic devices, electronic devices, optical fibers, electro-microfluidic systems, composite materials, fuel cells, indoor air-conditioning systems, active magnetic levitation systems and more. Some of the most recent numerical techniques, as well as some of the software among the most accurate and sophisticated in treating complex systems, are applied in order to exhaustively contribute in knowledge advances.

How to reference

In order to correctly reference this scholarly work, feel free to copy and paste the following:

Jovana Petrovic (2008). Modelling of Long Period Gratings in Photonic Crystal Fibres and Sensors Based on Them, Modelling and Simulation, Giuseppe Petrone and Giuliano Cammarata (Ed.), ISBN: 978-3-902613-25-7, InTech, Available from:

http://www.intechopen.com/books/modelling_and_simulation/modelling_of_long_period_gratings_in_photonic_crystal_fibres_and_sensors_based_on_them

INTECH
open science | open minds

InTech Europe

University Campus STeP Ri
Slavka Krautzeka 83/A
51000 Rijeka, Croatia
Phone: +385 (51) 770 447
Fax: +385 (51) 686 166
www.intechopen.com

InTech China

Unit 405, Office Block, Hotel Equatorial Shanghai
No.65, Yan An Road (West), Shanghai, 200040, China
中国上海市延安西路65号上海国际贵都大饭店办公楼405单元
Phone: +86-21-62489820
Fax: +86-21-62489821

© 2008 The Author(s). Licensee IntechOpen. This chapter is distributed under the terms of the [Creative Commons Attribution-NonCommercial-ShareAlike-3.0 License](#), which permits use, distribution and reproduction for non-commercial purposes, provided the original is properly cited and derivative works building on this content are distributed under the same license.

IntechOpen

IntechOpen